,

UNIVERSITY OF AMSTERDAM

Report

An In-depth Exploration of the SIR Model

October 1, 2024

Student:
Maarten Stork
2711760

Lecturer:
Mike Lees

Course:
Introduction to Computational Science

Course code:
5284ITCS6Y

Abstract

This paper explores the SIR (Susceptible-Infected-Recovered) model to enhance the understanding and management of infectious disease spread across diverse demographic settings. Through numerical simulations and theoretical analysis, we examined the impact of vaccination strategies, demographic dynamics, and infection-induced mortality on disease progression. The study also extended the Naive SIR model to incorporate variations such as seasonal effects, population turnover, and incubation periods, providing a more realistic framework for predicting disease behavior. The results showed that these modifications significantly improved the model's accuracy in forecasting disease dynamics and the timing of infection waves, offering more precise insights for epidemic control. These findings highlight the necessity of adapting models to accommodate real-world complexities rather than relying on (overly) simplified approaches.

Keywords: SIR model, infectious disease, numerical simulations, vaccination strategies, demographic changes, epidemic modeling, seasonality, infection-induced mortality, epidemiology.

Contents

1 Introduction

1.1 Motivation

Mathematical modeling serves as a fundamental tool in epidemiology, providing insights into the spread of infectious diseases across populations. Among these models, the Susceptible-Infected-Recovered (*SIR*) model stands out as a seminal framework in the field [9]. Developed in the early 20th century by Kermack and McKendrick, this model was one of the first to apply mathematical formulas to describe how diseases spread through human communities [10]. This interest in modelling diseases was truly sparked by the need to understand and predict the behavior of epidemics like the influenza pandemic of 1918 [8], the SIR model introduced a new approach by dividing the population into three distinct categories: those susceptible to infection, those infected, and those who have recovered and gained immunity.

This framework has since evolved, now able to model more complex interactions and reflect nuances of various real-world epidemiological scenarios. The adaptability of the base SIR model has not only solidified its theoretical foundation but has also increased its utility in practical disease-modelling. Today, it continues to be an extensively-used resource in epidemiology, helping public health officials and researchers predict and manage the dynamics of infectious diseases [8].

This paper explores the application of different types of SIR models through both numerical simulations and theoretical analysis, highlighting its role in crafting disease management strategies. As we explore the model's capabilities, we'll demonstrate how its adaptable framework could possibly aid in decoding future pandemics and help equip us for for these upcoming disease-related challenges, thereby sustaining its role as a pillar in epidemiological research.

1.2 Research Question

This study is guided by the overarching research question:

How can modifications to the Naive SIR model improve the understanding and management of infectious disease outbreaks?

This inquiry is further dissected into sub-questions corresponding to the three primary focuses of this paper:

(1) *How does the Naive SIR model describe the dynamics of an infectious disease, and what are the implications of various vaccination strategies on the model's predictions for epidemic control?*

This first subquestion, explored in Chapter 2, investigates the foundational Naive SIR model's ability to simulate the spread of an infectious disease and assesses the effectiveness of different vaccination strategies within this framework. The analysis aims to demonstrate how simple interventions can be modeled and quantified, thereby offering insights into the basic mechanisms of epidemic control. Understanding these fundamentals is essential for evaluating more complex models and strategies, thus laying the groundwork for addressing the overarching research question of improving epidemic management.

(2) *How does incorporating demographic factors and infection-induced mortality alter the predictions of the Generalized SIR model?*

This second subquestion, explored in Chapter 3, delves into a more complicated, but therefore more accurate, SIR Model by integrating demographic changes and mortality-due-to-infection. This extension aims to reflect more realistic scenarios where population dynamics significantly affect disease spread and outcome. By evaluating these factors, the chapter seeks to enhance our understanding of disease persistence and severity. The insights gained from this investigation contribute directly to the main research question by illustrating how model complexity can lead to a better general understanding of disease dynamics.

(3) *What are the dynamics and predictive capabilities of the SEIR Model on infection rates, and what does the addition of seasonal effects change?*

This third subquestion, explored in Chapter 4, assesses the impact of adding more stages to the Generalized SIR model (an *Exposed* class) and incorporating seasonal variations in transmission rates. The outcomes of this analysis will demonstrate the potential of adaptations of the base SIR Model to gain knowledge about both predictable seasonal outbreaks and less predictable pandemics, thereby directly addressing the overarching question of enhancing disease-related knowledge through refined modeling techniques.

Together, these questions are necessary for the exploration of the effectiveness and flexibility of the SIR model in varying epidemiological contexts and subsequently necessary for answering our main research question.

1.3 Methodology

This study utilizes a multi-faceted approach to explore the behavior of the SIR framework. The overarching goal is to evaluate the sensitivity of these models to various parameters and configurations.

At the core of the methodology is **Numerical Integration**, which is able to 'solve' the systems of ordinary differential equations that define the transitions between different groups in the population. It is important to note that it is technically not possibly to **Numerically Solve** these equations, due to the nonlinear transmission term, described in Chapter 1 of '*Modelling Infectious Diseases in Humans and Animals*' by Keeling&Rohani. We can, however, obtain an approximate solution for the "epidemic curve," which is defined as the number of new cases per time interval. To achieve this, Python's `scipy` library was used extensively, employing the `odeint` and `solve_ivp` functions to perform numerical integration across different time scales and parameter settings. These simulations were conducted for both epidemic and non-epidemic scenarios, with a focus on examining how changes in key parameters—such as the infection rate (β), recovery rate (γ), and death rates (μ and (ρ)) affect disease progression.

To visualize the behavior of these models, **Phase Plots** were generated to display the trajectories of susceptible and infected populations over time. Phase plots provide a graphical representation of how different initial conditions or parameter sets lead to varying epidemic outcomes. These plots were especially useful for illustrating the long-term behavior of the disease, particularly in terms of stability (whether the disease dies out, becomes endemic, or oscillates over time).

Oscillatory Analysis was another important focus of the analysis done in this paper. For models that exhibited periodic outbreaks, Fourier Transforms were employed to detect and analyze oscillations. **Fourier Analysis** allowed for the identification of peak frequencies and amplitudes in the infection dynamics, offering a clear understanding of the cyclical nature of diseases.

Scenario Analysis was done to examine the outcomes under different vaccination strategies, including multiple different vaccination strategies. These strategies were incorporated into the SIR model to simulate their effects on disease spread. By altering the structure of the SIR equations, the study could compare the outcomes of various intervention methods.

Additionally, **Sensitivity Analysis** was performed to determine how small changes in model parameters could lead to significant variations in the model's predictions. This analysis helped to identify certain critical thresholds (such as the basic reproduction number R_0).

Seasonality Analysis was also incorporated into the SEIR model by introducing a time-dependent transmission rate ($\beta(t)$) that oscillates according to seasonal changes. This approach allowed the study to simulate periodic disease outbreaks driven by environmental factors or changes in population behavior throughout the year. Finally, real-world epidemiological data from the 1978 influenza outbreak in a British boarding school was used for **Model Fitting**. This involved optimizing the transmission and recovery rates by minimizing the difference between model predictions and observed data, using Python's `scipy.optimize` module.

In summary, the study employed a comprehensive set of methods (numerical integration, phase plots,

Fourier analysis, sensitivity analysis, literature review, and real-world data fitting) to explore the dynamics of the SIR model, and its variations, under a variety of conditions.

1.4 Overview of Relevant Literature

In this sub-chapter, I will highlight two key pieces of literature that were indispensable in shaping the foundation of this paper. These texts provided the essential theoretical frameworks, practical methodologies, and insights necessary to carry out the research. While other sources were undoubtedly valuable, their contributions were more focused or specific, and as such, they will be cited in the general reference list rather than discussed in detail here.

(1) In *Modelling Infectious Diseases in Humans and Animals*, authors Matt J. Keeling and Pejman Rohani provide a beginners guide to the mathematical modeling of infectious diseases. The book goes into the fundamental principles of the SIR Model, offering both theoretical background and practical examples.

For this study, the book was particularly helpful in understanding the basic SIR framework and the various extensions that incorporate more and more real-world complexities, such as vaccination strategies and demographic effects. Its explanations of model formulation, numerical solutions, and interpretation of results were valuable in guiding the implementation and analysis of the models used in my own research. Additionally, the book's discussions on oscillations and endemic stability directly informed the analysis of periodic outbreaks observed in the simulations. Overall, Keeling and Rohani's work provided essential foundations for both the theoretical understanding and practical applications in the study.

(2) In *Nonlinear Dynamics and Chaos*, author Steven H. Strogatz offers a comprehensive exploration of the mathematical principles governing nonlinear systems, which are critical to understanding the behaviors in the ODE's of the SIR Model. Strogatz's treatment of phase plane analysis, bifurcations, and limit cycles was very welcome for framing the oscillatory behaviors and stability of equilibrium points in the models analyzed in this paper. Overall, Strogatz's work was essential in guiding the nonlinear analysis techniques employed in this study.

2 Naive SIR Model

This chapter will delve into the detailed mechanics of the Naive SIR model, starting with an explanation of its governing equations and progressing through practical applications that demonstrate its utility in understanding and managing infectious disease outbreaks. By integrating numerical simulations with real-world data analysis, we aim to showcase the model's adaptability in various epidemiological scenarios. The primary (sub)question guiding this section is:

(1) *How does the Naive SIR model describe the dynamics of an infectious disease, and what are the implications of various vaccination strategies on the model's predictions for epidemic control?*

2.1 Mathematical Framework

In this subchapter, we will dissect the Naive SIR model's mathematical framework to understand how infectious diseases propagate through the different SIR population segments.

The fundamental equations of the model are [10]:

$$\frac{dS}{dt} = -\beta SI \tag{1}$$

$$\frac{dI}{dt} = \beta SI - \gamma I \tag{2}$$

$$\frac{dR}{dt} = \gamma I \tag{3}$$

Equation (*1*) quantifies the rate at which susceptible individuals become infected. It is dependent on the rate of contact between susceptible and infected individuals, represented by β, and the number of interactions between these two groups, denoted by the product SI.

Equation (*2*) captures the change in the infected population. This equation increases with new infections (βSI) but decreases as infected individuals recover or become immune, at a rate γ, moving to the recovered category.

Equation (*3*) describes the rate at which infected individuals recover and gain immunity, thus transitioning to the recovered group. The term γI represents the recovery process, proportional to the current number of infected individuals.

The underlying assumption in these equations is that the total population ($N = S+I+R$) is constant, implying that the population is closed with no births, deaths (unrelated to the disease), immigration, or emigration. This assumption simplifies the model (hence, naive), allowing us to focus solely on the disease dynamics without external population influences.

Further analysis of the SIR model introduces the basic reproduction number, R_0, a critical epidemiological metric [10]. It is defined as the average number of secondary infections produced by a single infected individual in a completely susceptible population:

$$R_0 = \frac{\beta}{\gamma}$$

For an epidemic to emerge and sustain itself, R_0 must exceed 1, indicating that each infected individual, on average, transmits the disease to more than one other person [6]. This concept is important for understanding the spread and potential for an outbreak of an infectious disease.

The relationship between R_0 and the initial proportion of susceptible individuals, $S(0)$, is captured by the epidemic threshold phenomenon [10]. The critical condition for the infection to increase is:

$$\frac{dI}{dt} = \beta SI - \gamma I > 0 \Rightarrow S > \frac{\gamma}{\beta}$$

If $S(0)$ is less than $\frac{\gamma}{\beta}$, then $\frac{dI}{dt}$ becomes negative, leading to the infection dying out. Thus, the initial fraction of susceptibles must exceed this threshold, $\frac{\gamma}{\beta}$, for an epidemic to take hold in the population. This threshold has been originally noted in epidemiological studies such as those by Ransom (1880, 1881) and Hamer (1897), who explored the dynamics of disease spread and control [13, 6].

2.2 Numerical Integration

In this subchapter, we will employ numerical integration to explore two distinct scenarios in disease progression using the Naive SIR model, distinguished by their outcomes: one results in an epidemic, and the other does not. The determinant for each scenario's result is the basic reproductive number, $R_0 = \frac{\beta}{\gamma}$.

By fine-tuning the parameters β and γ, we manipulate R_0, allowing us to investigate its impact on the spread of an infectious disease. These parameters are varied to simulate conditions where R_0 exceeds or falls below the threshold of 1, marking the difference between epidemic outbreak and disease decline.

To visually capture and analyze the contrasting dynamics of the epidemic and non-epidemic scenarios, we'll present two diagrams; one for an epidemic scenario and one for a non-epidemic scenario. Next to these, we will present Fourier Transforms and Phase Plots for each scenario. These diagrams together track the proportions of susceptible, infected, and recovered individuals over time, showcasing how shifts between these states occur under different R_0 conditions.

2.2.1 Epidemic Scenario

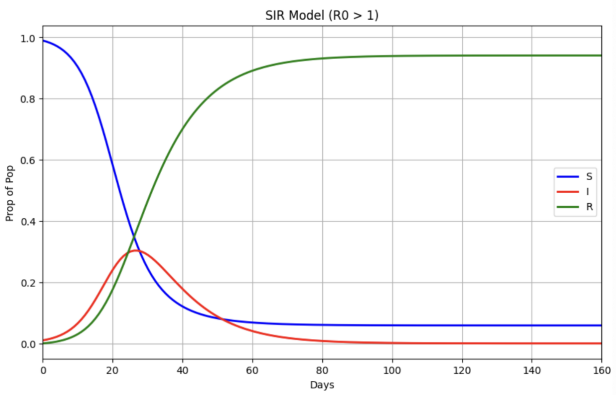

Figure 1 *Naive SIR - Epidemic scenario with* $R_0 > 1$.

Figure 1 depicts a scenario where $R_0 > 1$, meaning a scenario where an infected individual transmits the disease to more than one person on average. In this simulation, the transmission rate (β) is set to 0.3, and the recovery rate (γ) is set to 0.1, resulting in $R_0 = 3$. The values for (β) and (γ) have been chosen semi-randomly, with the only criteria being to ensure the

value of $R_0 > 1$. The resulting dynamics show a rapid increase in the infected population, which peaks before gradually declining as susceptible individuals become infected and then recover. This curve illustrates the typical behavior of an epidemic where the infection spreads widely before control measures and natural immunity reduce transmission [18].

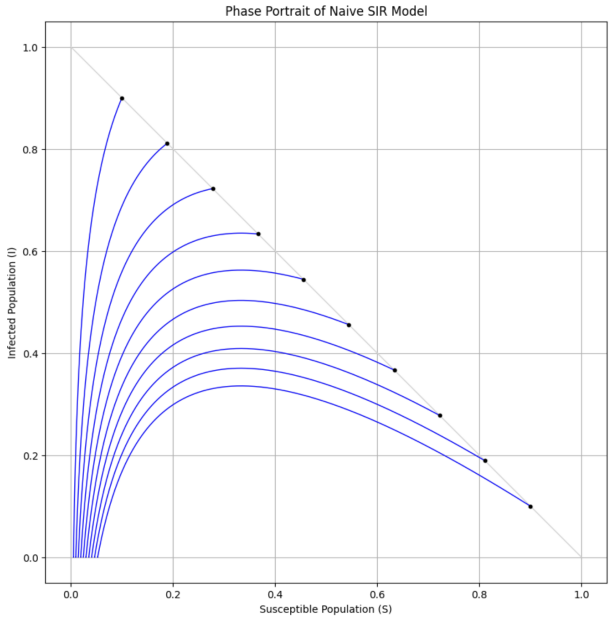

Figure 2 figure
Phase Plot Naive SIR - Epidemic scenario with $R_0 > 1$.

Unlike more sophisticated models (incorporating seasonal or demographic factors, which are both discussed in *Chapter 3* and *Chapter 4* respectively), there are no oscillations present in the Naive SIR model, depicted in *Figure 2*. This is backed up by academic literature, like Weiss (2013), who highlights that while the Naive SIR model provides useful insights into disease dynamics, it lacks the capability to account for oscillatory behavior often observed in real-world epidemiological data due to its simplified assumptions about constant transmission rates and homogeneous populations [18]. The phase plot of the Naive SIR Model when $R_0 > 1$ exhibits a steady slightly-curved trajectory towards the zero-point rather than showing periodic fluctuations in the number of infected individuals. The trajectory simply converges toward the extinction of the infection, indicating that the disease will die out.

2.2.2 Non-Epidemic Scenario

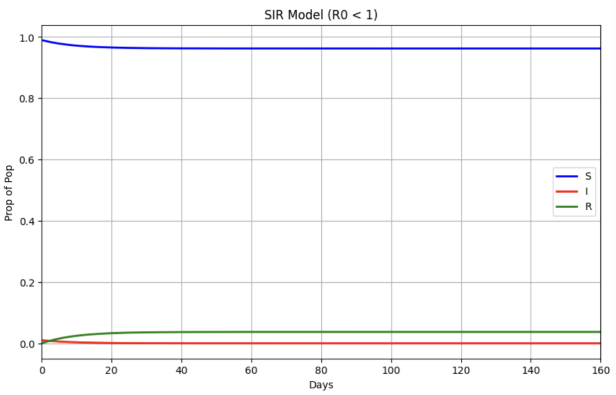

Figure 3 *Naive SIR - Epidemic scenario with* $R_0 < 1$.

Figure 3 illustrates the scenario when $R_0 < 1$, indicating a non-epidemic scenario. Here, the transmission rate (β) remains at 0.3, but the recovery rate (γ) is increased to 0.4, resulting in $R_0 = 0.75$. The values for (β) and (γ) have been chosen semi-randomly, with the main criteria being to ensure the value of $R_0 < 1$. This adjustment leads to insufficient transmission to sustain the spread of the infection. The infected population initially increases slightly but quickly diminishes, demonstrating how a higher recovery rate can prevent an epidemic from taking hold in the population.

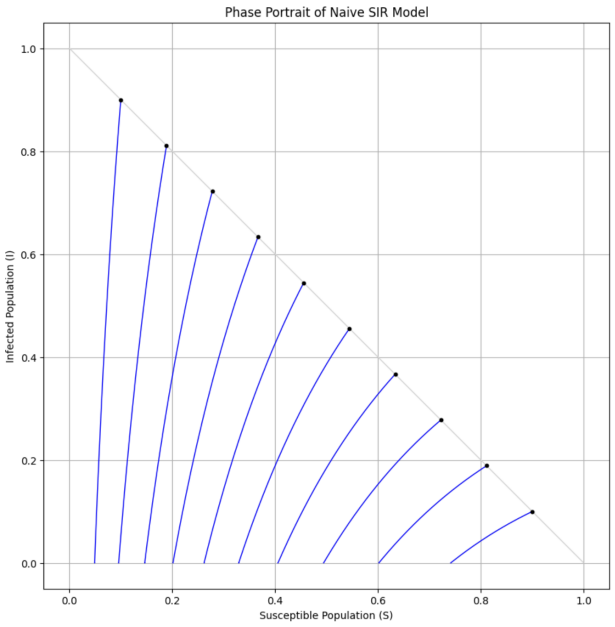

Figure 4 *Phase Plot Naive SIR - Epidemic scenario with* $R_0 > 1$.

Just like the epidemic scenario, the non-epidemic trajectory in *Figure 4* shows a fast convergence to zero infected individuals. The trajectories demonstrate that the infection fails to persist in the population when $R_0 < 1$, leading to a quick decline in the number of infected individuals and an eventual extinction of the disease (at an even quicker rate than when $R_0 > 1$).
Just like in the epidemic scenario (in *Chapter 2.2.1*), there are no oscillations present in the Naive SIR model under non-epidemic conditions [18]. The infection spreads briefly but fails to establish itself, and the system converges to a steady state where the disease has disappeared entirely. This result confirms that in the absence of sufficient transmission ($R_0 < 1$), the infection will die out, leaving the susceptible population unaffected.
These figures depicted in *Chapter 2.2.1* and *Chapter 2.2.2* provide a visual depiction of how variations in β and γ affect the spread of infectious diseases, demonstrating the threshold effect of R_0 on disease outcomes.

2.3 Real World Data Application

By applying the Naive SIR model to historical data from an influenza outbreak in a boys' school, we can estimate the infection and recovery rates. We obtained this data directly from Chapter 2.5 of the '*Modelling Infectious Diseases in Humans and Animals*' by Keeling&Rohani [11]. This analysis not only illustrates how the Naive SIR Model can be fitted to real data but also shows how it can be used to forecast disease progression in real-world scenarios.
During the early weeks of the Easter term in 1978, an outbreak of influenza A virus (A/USSR/90/77 (H1N1)) occurred in a British boarding school, rapidly affecting a large portion of the student body [11]. Out of 763 boys, many contracted the illness within a short period, making this scenario an ideal case study for applying the Naive SIR model.
To fit the Naive SIR model to the exact data of the outbreak, we used Python's `scipy` library, particularly the `solve_ivp` function to solve the SIR system of equations, and the `minimize` function from the same library to optimize the transmission and recovery rate. By minimizing the difference between the model's predictions and the historical data points, we could estimate these parameters. Our objective was to reduce the squared errors between the number of infected individuals predicted by the model and the observed data for each day.
Figure 5 above shows the original data of the outbreak alongside the fitted values generated by the Naive SIR model.

Day	Historical Data	Model-Fitted Data
0	1	1
1	3	3
2	8	11
3	28	35
4	75	98
5	221	206
6	291	283
7	255	275
8	235	222
9	190	164
10	125	116
11	70	80
12	28	54
13	12	37
14	5	25

Figure 5 *Table with the Data of an Influenza Outbreak*

In *Figure 6*, we further visualize the model's fitted curves, plotted alongside the original data points. The close alignment between the SIR model's infection curve and the actual data suggests a good fit, demonstrating how model parameters can reflect the real-world spread of the disease.

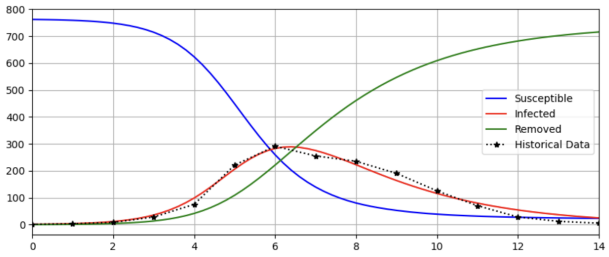

Figure 6 *Model of the Data of an Influenza Outbreak*

By minimizing the sum of squared differences between the model's predictions and the historical data, we estimated the transmission rate $\beta \approx 1.67$ and recovery rate $\gamma \approx 0.45$, yielding an R_0 of approximately 3.72. These parameter estimates provide an approximation of the disease spread in the boys' school, indicating that on average, each infected individual was able to spread the virus to three-to-four others, resulting in the rapid spread of the infection you can see in the data.

2.4 Vaccination Strategies

Finally, we will design and evaluate potential vaccination strategies. This involves hypothesizing two different vaccination scenarios, simulating their impacts using the Naive SIR model, and comparing their efficacy in controlling the disease spread. This subsection will demonstrate the model's applicability in planning and optimizing vaccination campaigns, solely focusing on the control strategy of vaccination, instead of the wider ranger of control strategies discussed in Chapter 1 of '*Modelling Infectious Diseases in Humans and Animals*' by Keeling&Rohani.

2.4.1 Ring Vaccination Strategy

The Ring Vaccination Strategy employs a targeted approach where vaccinations are given to individuals who are in close contact with infected people [19]. This strategy effectively creates a 'ring' of immunity around each infected individual, preventing the spread of the disease to the wider community. Historically, this strategy has been successful in controlling outbreaks of smallpox [5] and is currently applied in managing Ebola virus outbreaks [16]. The success of this strategy depends on the rapid detection of cases and the rapid deployment of vaccinations to contacts of the infected.

For the Ring Vaccination Strategy, our null hypothesis (H_0) would be that:

The Ring Vaccination Strategy implementation significantly reduces the transmission of infections by containing potential outbreaks within immediately affected groups.

To test this, we would simulate an outbreak in a model of a closed community (such as a school, referring back to *Chapter 2.3*), starting with a single infected individual. We would model different scenarios varying the speed of vaccination deployment and the definition of who qualifies as a close contact. The effectiveness of this strategy would be measured by comparing the total number of infections, the peak infection rate, and the outbreak duration against a no-vaccination scenario [19].

Subsequently, we would need to perform these tests in a test-environment such as the Naive SIR Model. Implementation of this in the Naive SIR model would involve adjusting the dynamics of the susceptible group after the identification of an infection. Vaccinating a "ring" of close contacts to the infected would mean in Naive SIR that a portion of the susceptible individuals within the vicinity of the infected person would be removed from the susceptible category and transferred directly to the recovered category without passing through the infected state [17].

When simulating this strategy within the Naive SIR model, we would need to track several key metrics to evaluate its impact. Firstly, (*1*) we would record the number of susceptible individuals who are vaccinated and thus directly transitioned to the recovered status without undergoing infection. This step is necessary as it reduces the susceptible pool immediately surrounding each detected case. Additionally, (*2*) we would monitor the speed of this vaccination process following case detection, which critically affects how rapidly the susceptible population decreases. Finally, (*3*) the effectiveness of this strategy would be observed

in the reduction of the peak infection rate, demonstrating how efficiently the outbreak is being contained by preventing new infections among those at highest risk. This approach ensures that the simulation captures the dynamics of disease spread and the direct effects of intervention measures.
The impact of varying the definition of "close contact" (the radius of vaccination coverage) would be seen in the size of the vaccinated group within the SIR model [17]. Larger coverage would lead to more individuals moving from S to R, effectively lowering the infection spread more rapidly [4].
The comparison to the no-vaccination scenario would (at least according to our null hypothesis) demonstrate how ring vaccination flattens the infection curve and shortens the outbreak duration by limiting the available pool of susceptible individuals who can be infected.

2.4.2 Contact Network Strategy

The Contact Network Strategy targets individuals based on their centrality within a community's network, aiming to disrupt the transmission chain at its largest spreaders [12]. This approach identifies individuals who, because of having a lot of different connections, are most likely to spread the infection widely. This strategy can be very useful in densely connected populations like schools or workplaces and relies on detailed data on social interactions to be effective [14].
A notable application of this strategy was during the COVID-19 pandemic. North-American researchers used contact tracing and movement data to identify highly connected individuals (those who frequented multiple locations or had many contacts) and prioritized them for vaccination. For instance, a study conducted by RAND analyzed Northern-American citywide movement patterns to locate individuals with high centrality in the contact network. By vaccinating these individuals first, they were able to control the epidemic more rapidly than through random vaccinations, demonstrating the efficiency of this strategy [4].
For the Contact Network Strategy, our null hypothesis (H_0) would be that:

Vaccinating individuals based on their network centrality leads to a more efficient reduction in the spread of infection compared to non-targeted vaccination strategies.

To test this, we would simulate an outbreak in a networked model of a school, where nodes would represent individuals and edges would represent close contacts. We would start the simulation with a few randomly infected nodes and apply vaccination selectively based on various measures of centrality [17]. The strategy's performance would be evaluated by analyzing the number of infections, the time to peak, and the outbreak duration, comparing these results with those from other vaccination strategies.
Implementing this strategy in the SIR model would require incorporating additional data about the network structure of the school population [17]. Each individual (node) would have varying numbers of connections (edges), and those with the highest number of edges would be prioritized for vaccination. In the SIR framework, this involves removing those most highly connected individuals from the susceptible group (S) and transferring them to the recovered group (R), thereby preemptively preventing them from serving as major transmission vectors.
In the simulation of the Contact Network Strategy within the SIR model, the impact of the strategy would be kept track of and analyzed to assess its effectiveness. Firstly, (*1*) the process would involve observing how the removal of high-contact individuals influences the transmission dynamics in the overall population. This would particularly focus on any reductions in the transmission rate, which should be expected as the biggest spreaders would get vaccinated. Secondly, (*2*) the simulation would monitor changes in the infection curve, specifically looking for reductions in the number of infections and changes in the time to peak infection rates, which indicate the effectiveness of the vaccinations on the network's most popular people. Finally, (*3*) the outcomes of these targeted vaccinations would be compared with results from scenarios

where no vaccination or where a random vaccination is implemented. This comparison aims to highlight the efficiency of targeting central nodes in the network, demonstrating how such a strategic approach can more effectively reduce the spread of the disease compared to less focused methods [4].

Both the Ring Vaccination and the Contact Rate strategies utilize the base principles of the Naive SIR model to predict and control the flow of infections, and adapting the model parameters based on the strategy employed should accurately visualize the potential outcomes of these interventions. This underlines the usefulness of the Naive SIR Model, especially in disease-scenarios where the need for testing without real-life harm is enormous.

3 Generalized SIR Model

This chapter extends the analysis of the Naive SIR model by incorporating demographic factors such as birth and natural death rates (resulting in the Generalized SIR Model), as well as infection-induced mortality. These modifications allow for a more realistic simulation of infectious disease dynamics over extended periods and in populations with demographic changes [10].

The primary (sub)question guiding this section is:

(2) *How does incorporating demographic factors and infection-induced mortality alter the predictions of the Generalized SIR model?*

3.1 Mathematical Framework

In this subchapter, we will explore the Generalized SIR model which incorporates additional demographic factors (birth and natural death rates) as well as infection-induced mortality. This expansion of the Naive SIR model allows for a more realistic simulation of infectious disease dynamics. The modified equations of the Generalized SIR model are [10]:

$$\frac{dS}{dt} = \mu - \beta SI - \mu S \tag{1}$$

$$\frac{dI}{dt} = \beta SI - \gamma I - \mu I \tag{2}$$

$$\frac{dR}{dt} = \gamma I - \mu R \tag{3}$$

Equation (1) now includes a term μ representing the birth rate into the susceptible population, and μS, the natural death rate of the susceptible individuals. The infection rate remains influenced by β, the contact rate, and SI, the interaction term between susceptible and infected individuals.

Equation (2) reflects the rate of change in the infected population, considering both the new infections and the losses due to recovery (γI) and natural death (μI). This equation highlights the dynamic balance between disease transmission and recovery or death.

Equation (3) now includes a death rate μR for the recovered individuals, in addition to them acquiring immunity through recovery at rate γ.

Similar to the Naive SIR Model, in Chapter 2, this model assumes a constant population size ($N = S + I + R$) with equal birth and death rates, simulating natural population turnover [10].

Despite these additions, the critical dynamics of the disease spread can still be captured by the basic reproduction number R_0, now adjusted for the death rate:

$$R_0 = \frac{\beta}{\gamma + \mu}$$

This formulation highlights that the disease's ability to invade (and persist) in the population depends not only on the transmission and recovery rates but also significantly on the rate of demographic turnover. The threshold condition for the endemic existence of the disease, where the infection becomes stable and persistent without leading to eradication or explosion, can be further explored through the stability analysis of the model [6].

3.2 Numerical Integration

This subchapter employs numerical integration to explore the dynamic responses of the Generalized SIR model under the influence of demographic factors such as birth and natural death rates, as well as disease-induced mortality. This model allows us to understand how these factors contribute to the disease becoming endemic or causing oscillatory patterns in the population.

To investigate these dynamics, we simulate two scenarios using numerical integration: one where the basic reproductive number R_0 is greater than one, indicative of an epidemic potential, and another where R_0 is less than one.

3.2.1 Epidemic Scenario

In the epidemic scenario, our simulations utilize the parameters $\beta = 0.3$, $\gamma = 0.1$, and $\mu = 0.01$. This gives $R_0 = \frac{0.3}{0.1+0.01}$, which means $R_0 \approx 2.72$.

The Generalized SIR Model with these parameters has been depicted in *Figure 7*, where the addition of a constant birth and death rate shows a dynamic equilibrium, meaning the disease becomes endemic rather than being eradicated. This results in oscillatory patterns of infection over time, indicating a continuous, although not explosive, spread of the disease across the population [11]. These oscillations are quantified through Fourier Analysis shown in *Figure 8*, which identifies a peak frequency of approximately 0.006 cycles per day and a peak amplitude of about 11.7, suggesting periodic fluctuations in infection levels [3].

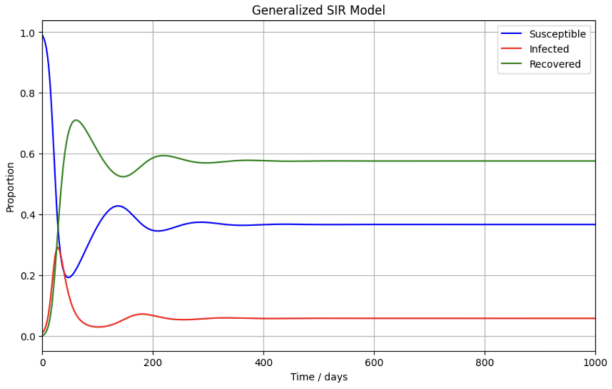

Figure 7 *Generalized SIR - Epidemic scenario with* $R_0 > 1$.

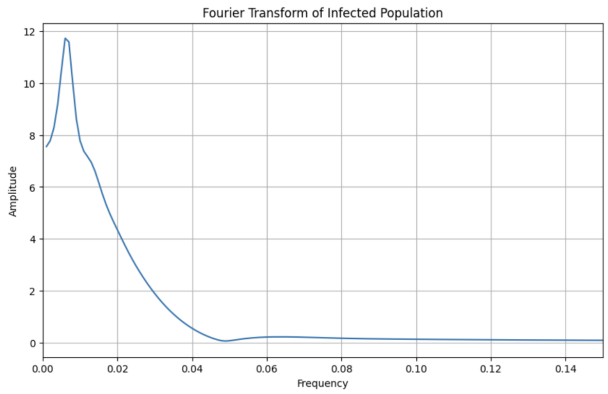

Figure 8 *Fourier Transform Generalized SIR - Epidemic scenario with* $R_0 > 1$.

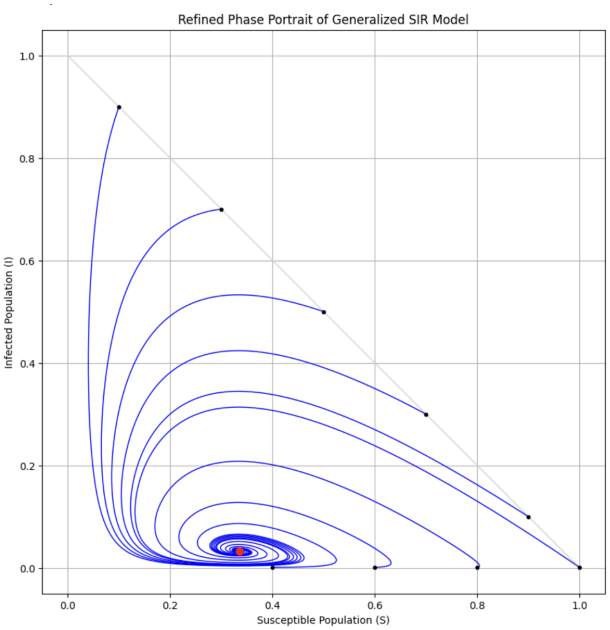

Figure 9 *Phase Plot Generalized SIR - Epidemic scenario with* $R_0 > 1$.

The phase portrait, as illustrated in *Figure 9*, shows trajectories in the space of susceptible and infected proportions, indicating how the population cycles through periods of higher and lower infection rates before stabilizing. These trajectories describe a path toward endemic stability, spiraling into a fixed point where the disease remains present but controlled.

3.2.2 Non-Epidemic Scenario

In contrast, *Figure 10* depicts the non-epidemic scenario where ($R_0 < 1$), leading to quick extinction of the disease. The Fourier Transform for this scenario, as shown in *Figure 11*, reveals much lower amplitude os-

cillations (a (peak) frequency of approximately 0.001 cycles per day and a (peak) amplitude of about 0.14), which taper off quickly, indicating the disease's inability to establish itself within the population.

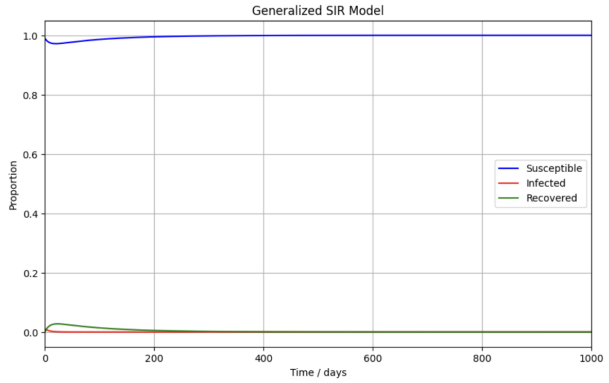

Figure 10 *Generalized SIR - Non-Epidemic scenario with* $R_0 < 1$.

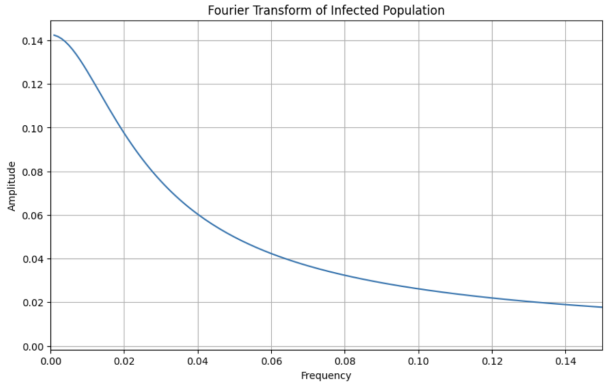

Figure 11 *Fourier Transform Generalized SIR - Non-Epidemic scenario with* $R_0 < 1$.

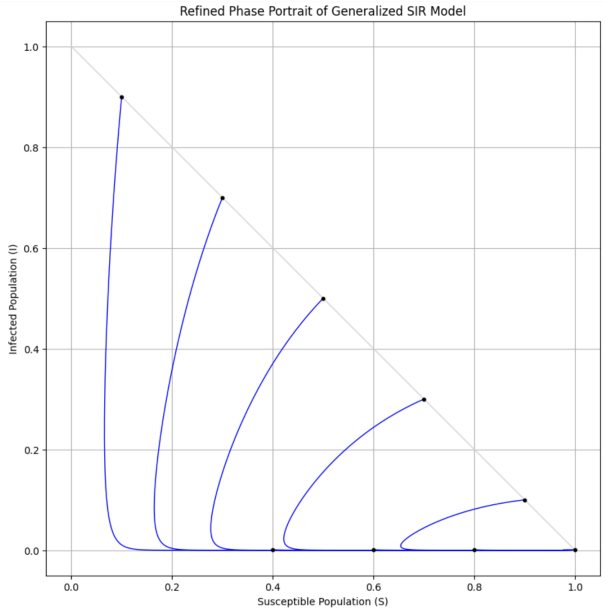

Figure 12 *Phase Plot Generalized SIR - Non-Epidemic scenario with* $R_0 < 1$.

The phase portrait for the non-epidemic scenario, shown in *Figure 12*, highlights a trajectory where the disease does not spread, and everyone eventually succumbs to natural causes, returning to the susceptible population. This means that over time, both the infected (I) and recovered (R) populations decrease, ultimately leaving the entire population in the susceptible (S) category.

The phase portrait also reveals several fixed points, indicating equilibrium states where the populations remain constant. The fixed point at $S = 1$ and $I = 0$ represents the disease-free equilibrium, where the infection has completely disappeared from the population. Other trajectories spiral or converge toward these equilibrium points, showing how the infection gradually declines in the population. This behavior is typical in models where no oscillations are present, confirming that the infection will die out under these conditions [11].

The findings gained by modelling both the epidemic and non-epidemic scenarios with the Generalized SIR Model underscore the nuanced behavior of infectious diseases when demographic dynamics are considered, revealing the impact of natural population processes on disease propagation when compared to the Naive SIR Model, discussed in *Chapter 2* of this paper [7].

3.3 Infection-Induced Mortality

The Generalized SIR Model in its current form however lacks accuracy. It does not fully account for the dynamics of the Infected class, where changes are driven not only by natural births and deaths but also by mortality due to the infection itself. In this subchapter, we will address these dynamics by modifying our established Generalized SIR Model to include infection-induced mortality.

We can incorporate this feature in two different ways. The first approach involves using a separate mortality rate. This method, while somewhat oversimplified, provides a useful basis for discussion [10]. The second approach combines both mortality and recovery rates into a single parameter, offering a more integrated perspective on the process [10]. For both approaches we will assume that ($N = S + I + R$) is not constant.

3.3.1 Separate Mortality Rate

For this strategy, we adjust the Generalized SIR Model equations as follows:

$$\frac{dS}{dt} = \mu - \beta SI - \mu S \tag{1}$$

$$\frac{dI}{dt} = \beta SI - \gamma I - \mu I - \rho I \tag{2}$$

$$\frac{dR}{dt} = \gamma I - \mu R \tag{3}$$

As illustrated, the primary modification is the inclusion of the term ρI in the second equation. This new term, ρ, represents the infection-induced mortality rate, capturing the rate at which infected individuals die specifically from the disease, distinct from natural mortality.

Numerically integrating these equations using the previously established values for β (0.3), γ (0.1), and μ (0.01), and introducing varying (increasing) values of ρ, illustrates the impact of increased infection-induced mortality on the dynamics of the Extended Generalized SIR Model, as depicted in *Figures 13*, *14*, and *15*. *Figure 13* depicts the dynamics of a generalized SIR model incorporating an infection-induced mortality term, with a mortality rate (ρ) set at 0.01.

From the graph, the Susceptible population experiences a sharp initial decline, indicating a rapid spread of the infection. This is followed by a stabilization near a proportion of 0.4, suggesting that a significant portion of the population remains susceptible, after the initial outbreak.

The Infected population initially peaks sharply, reflecting a fast increase in cases, before declining steadily. This indicates that the infection spreads quickly but is also overcome at a similar rate, either by recovery or death, leading to a decrease in active cases over time.

The Recovered population increases progressively, as expected, illustrating the recovery of individuals from the infection. This steady increase paired with the sharp decline in infections suggests effective recovery or immunity development among those infected. In summary, despite the low mortality rate of 0.01, the infection induces significant initial morbidity but transitions into a state where a large fraction of the population remains susceptible, the number of active infections declines, and recoveries accumulate over time. This portrays a scenario where the infection persists at a low level within the population, likely due to the continuous presence of a susceptible reservoir and the gradual process of recovery [15].

Figure 13 *Extended Generalized SIR - Epidemic Scenario with* $\rho = 0.01$.

In *Figure 14*, we observe the dynamics when the infection-induced mortality rate, ρ, is increased to 0.1. This adjustment leads to less of a peak in the Infected population, as a higher mortality rate more rapidly causes deaths in the number of active cases. The Susceptible population stabilizes at a higher level com-

pared to scenarios with a lower ρ, indicating that the disease is removing individuals from the population faster than they can be infected. The Recovered population's growth rate slows down compared to *Figure 13*, as relatively more individuals die from the infection rather than recovering. This model demonstrates how taking ten times the size of the mortality rate can lead to a significant change in the epidemic's progression, potentially shortening the duration of the outbreak but with a higher death count [15].

Figure 14 *Extended Generalized SIR - Epidemic Scenario with* $\rho = 0.1$.

Figure 15 depicts a dramatic impact on the epidemic dynamics with $\rho = 0.99$. In this graph, the Infected population almost immediately begins its decline to the endemic zero shortly after the outbreak begins. The Susceptible population remains virtually unchanged near its initial value, as the infection has a negligible chance to spread before infected individuals find their death. The Recovered population remains extremely low throughout the simulation, reflecting the deadly outcome for nearly all infected individuals. This setup illustrates the impact of a high disease-related mortality rate (of 99%), effectively stopping the epidemic's spread immediately by removing the infected individuals from the population after they contract the disease [10].

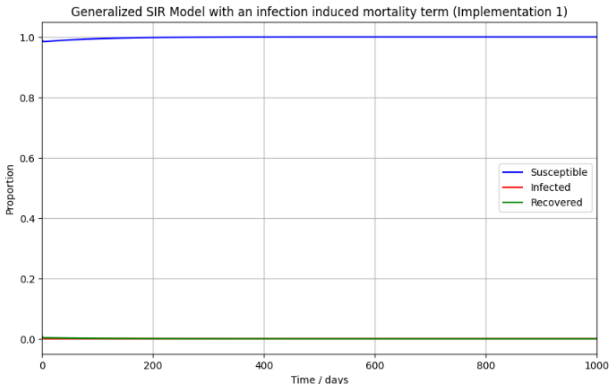

Figure 15 *Extended Generalized SIR - Epidemic Scenario with* $\rho = 0.99$.

3.3.2 Combined Mortality and Recovery Rates

For this second, more nuanced, strategy, we further adjust the Generalized SIR Model by combining the mortality and recovery rates into a single term within the equations [10]. The modified equations are expressed as follows:

$$\frac{dS}{dt} = \mu - \beta SI - \mu S \tag{1}$$

$$\frac{dI}{dt} = \beta SI - \left(\frac{\gamma + \mu}{1 - \rho}\right) I \tag{2}$$

$$\frac{dR}{dt} = \gamma I - \mu R \tag{3}$$

This configuration introduces a modified term in the infection equation, where the combined effects of μ, γ, and ρ are balanced against the total infected population.

Numerically integrating these revised equations with the established parameters for β (0.3), γ (0.1), and μ (0.01), and a varying ρ, provides insights into how changes in the infection-induced mortality rate can influence the dynamics of the epidemic. The resulting simulations, illustrated in *Figures 16*, *17*, and *18*, demonstrate the model's capability to depict different epidemic scenarios.

Figure 16 shows the epidemic scenario with $\rho = 0.01$ under the combined mortality and recovery rates implementation. In this graph, we observe a more dynamic fluctuation in both the Susceptible and Recovered populations compared to previous models. The low infection-induced mortality rate allows the infection to persist for a longer period, leading to oscilla-

tions in the number of susceptible individuals. This pattern arises because the mortality and recovery effects are now intertwined, causing more complex interactions within the population dynamics [15].

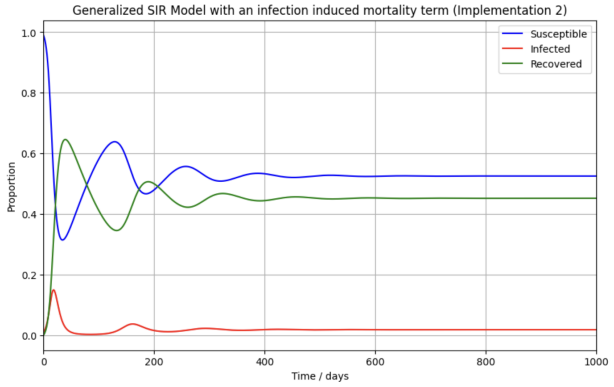

Figure 16 *Extended Generalized SIR - Epidemic Scenario with* $\rho = 0.01$.

Figure 17 presents the epidemic dynamics with a ρ of 0.1, where the combined mortality and recovery rates lead to less of a peak in the Infected population and a more stabilized Susceptible and Recovered population compared to *Figure 16*. Additionally, the higher mortality rate reduces the number of new infections, showing less fluctuation and a slower increase in the Recovered population, as relatively more individuals exit the model instead of continuing on to this Recovered population. This shows how intertwining mortality with recovery in our Generalized SIR Model can dampen epidemic peaks and extend the timeline of the Infection [10].

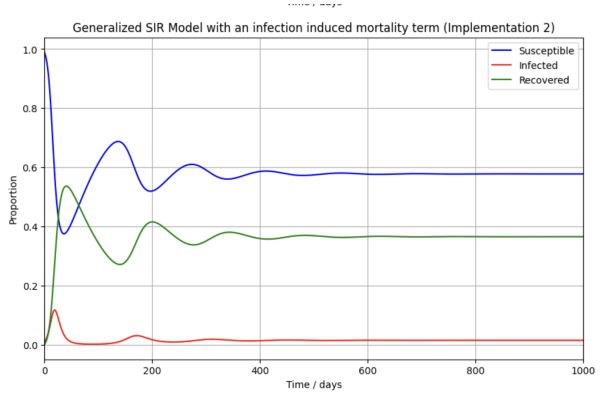

Figure 17 *Extended Generalized SIR - Epidemic Scenario with* $\rho = 0.1$.

Figure 18 illustrates the epidemic dynamics when the infection-induced mortality rate, ρ, is set to 0.99 within the combined mortality and recovery rates framework. In this extreme case, the Infected population immediately declines to nearly zero as soon as the outbreak begins, due to the overwhelming mortality rate. As such, the Susceptible population remains nearly constant, as the infection is swiftly fatal, preventing any significant transmission. The Recovered population remains minimal throughout the simulation, indicating that nearly no one survives the infection to enter the Recovered class.

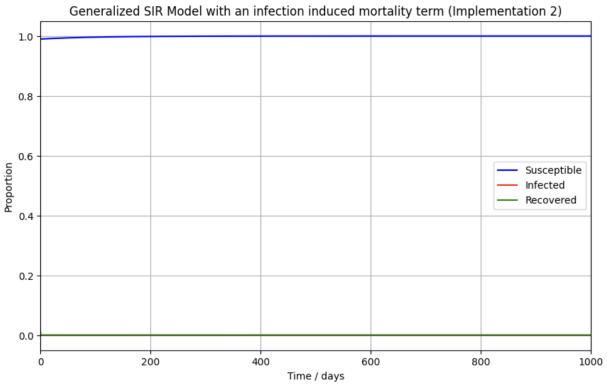

Figure 18 *Extended Generalized SIR - Epidemic Scenario with* $\rho = 0.99$.

The comparison between the separate and combined mortality and recovery rate models in the Generalized SIR framework reveals certain dynamics in how epidemics unfold. The separate model tends to show more pronounced fluctuations in population dynamics as mortality and recovery are treated as distinct processes. In contrast, the combined model generally exhibits smoother transitions and more stabilized populations, as it integrates the effects of mortality and recovery into a single rate, moderating the impact on the infected class. However, when both models increase the infection-induced mortality rate (ρ) (close) to 1.0, the outcomes converge, resulting in an immediate decline of the Infected population and minimal changes in the Susceptible and Recovered populations. This demonstrates that at extreme mortality rates, the structural differences between the models become almost negligible.

4 SEIR Model

This chapter extends the analysis of the Naive SIR model by introducing the SEIR model with demography, which includes an additional 'Exposed' compartment representing individuals who have been infected but are not yet infectious [10]. This refinement allows for the incorporation of an incubation period of a disease, as is the case with many different diseases.
The primary (sub)question guiding this section is:

(3) *What are the dynamics and predictive capabilities of the SEIR Model on infection rates, and what does the addition of seasonal effects change?*

4.1 Mathematical Framework

The mathematical formulation of the SEIR model with demography is given by the following differential equations [17]:

$$\frac{dS}{dt} = \mu - (\beta I + \mu)S \tag{1}$$
$$\frac{dE}{dt} = \beta SI - (\mu + \sigma)E \tag{2}$$
$$\frac{dI}{dt} = \sigma E - (\mu + \gamma)I \tag{3}$$
$$\frac{dR}{dt} = \gamma I - \mu R \tag{4}$$

Equation (1) includes a term μ, representing both the birth rate into the susceptible population and the natural death rate of susceptible individuals. The infection rate β affects the transition of individuals from susceptible (S) to exposed (E), based on their interaction with infectious individuals (I).
Equation (2) captures the dynamics of the exposed class E, transitioning into the infectious class at rate σ, while also subject to natural death, reflecting the incubation period where individuals are infected but not yet infectious.
Equation (3) describes the change in the infectious population, considering the influx from the exposed class and the losses due to recovery at rate γ and natural death at rate μ, representing the active phase of the disease.
Equation (4) is still the same, as a death rate μR is included, alongside the recovery process at rate γ, where individuals gain immunity.
As with the Generalized SIR Model, this framework supports the analysis of the basic reproduction number R_0, now nuanced by the additional transitions and the demographic influences:

$$R_0 = \frac{\beta}{\gamma + \mu}$$

This adjusted R_0 provides insights into the disease's potential to spread within the population, considering both the infection dynamics and the underlying demographic structure [10]. For this approach we will assume that ($N = S + I + R$) is not constant, similarly to our assumption in *Chapter 3* of this paper.

4.2 Numerical Integration

In this subchapter, we will perform numerical integration to explore the dynamics of the SEIR model with demography. We simulate two key scenarios: one where $R_0 > 1$, representing an epidemic situation, and another where $R_0 < 1$, leading to the extinction of the disease.

4.2.1 Epidemic Scenario

In the epidemic scenario, the transmission rate (β) is set to 0.3, the recovery rate (γ) is set to 0.1, and the birth/death rate (μ) to 0.01, resulting in $R_0 \approx 2.72$. This is illustrated in *Figure 19*, where the introduction of birth and death rates sustains the population at least for some time, allowing the infection to persist over time.
The addition of the Exposed class (E), a key feature of the SEIR model, captures the delay between infection and the onset of infectiousness [2]. Oscillatory behavior can be observed in all groups of the population, indicating recurring waves of infection over a prolonged period. The Exposed class provides a buffer, allowing the infection to build up before it becomes infectious, thereby influencing the timing and magnitude of infection 'waves'. These oscillations are further analyzed using a Fourier Transform, shown in *Figure 20*,

which reveals a peak frequency of ≈ 0.007 cycles per day and an amplitude of ≈ 157, demonstrating periodic outbreaks in the population.

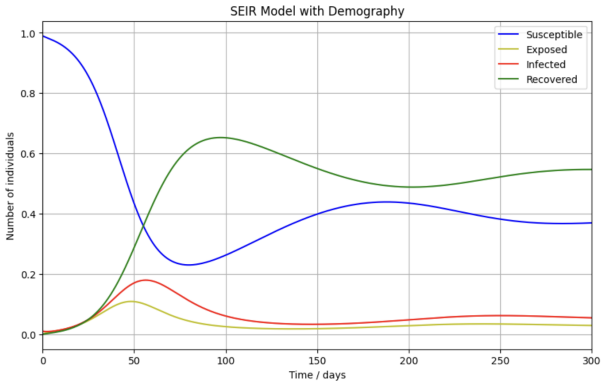

Figure 19 *SEIR Model with Demography - Epidemic scenario with* $R_0 > 1$.

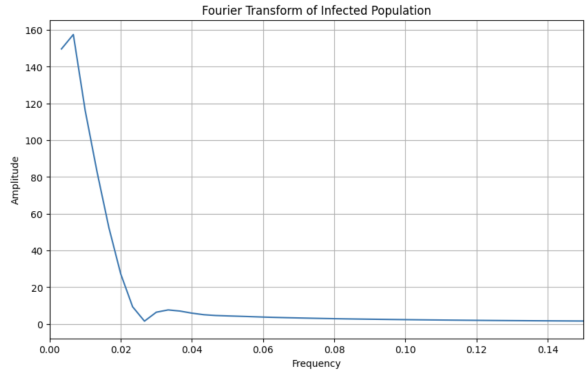

Figure 20 *Fourier Transform SEIR Model - Epidemic scenario with* $R_0 > 1$

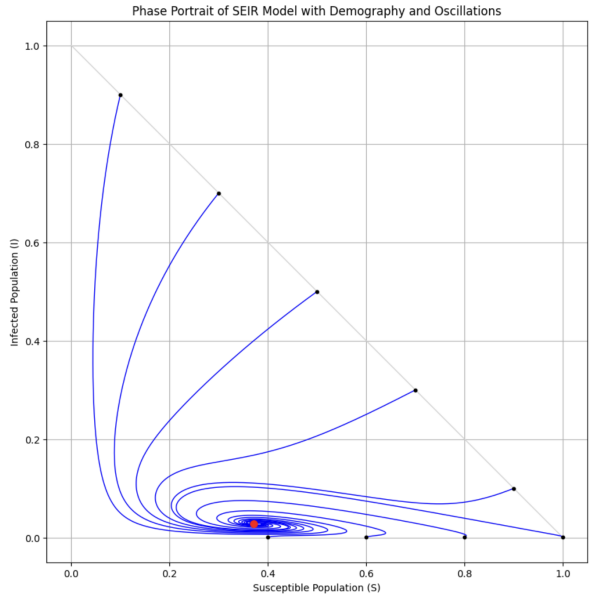

Figure 21 *Phase Portrait SEIR Model - Epidemic scenario with* $R_0 > 1$

The phase portrait in *Figure 21* demonstrates the trajectory of the susceptible, exposed, and infected populations over time, with spiraling paths that eventually converge to an endemic equilibrium. This stable point indicates that the disease persists in the population without being eradicated or flaring up massively. The Exposed class plays a crucial role in changing the disease's persistence, as the delay in the starting of infectiousness-states alters the dynamics compared to the simpler SIR model(s) [2], making the oscillations and eventual equilibrium stand out more. This is also noticeable in the trajectory of the oscillations, as they do not instantly spiral inwards like we expected to see based on our Phase Portraits for epidemic-scenarios in *Chapter 2* and *Chapter 3*, but rather extend straight inwards for a bit before spiralling.

4.2.2 Non-Epidemic Scenario

On the other hand, in the non-epidemic scenario where $R_0 < 1$, the transmission rate (β) is set to 0.3, the recovery rate (γ) is set to 0.4, and the birth/death rate (μ) to 0.01, $R_0 \approx 2.72$. As shown in *Figure 22* the infection quickly dies out as the number of susceptible individuals remains high, and both exposed and infected populations decline toward zero. The Fourier Transform of this scenario, depicted in *Figure 5*, shows lower oscillation frequencies (≈ 0.0003) and amplitudes (≈ 5.28), confirming that the disease fails to establish a stable cycle of infection in the population.

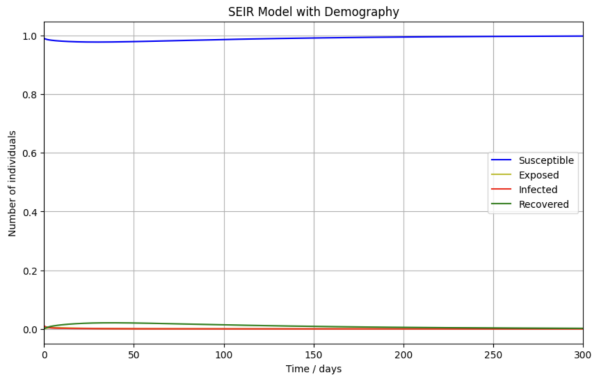

Figure 22 *SEIR Model with Demography - Non-Epidemic scenario with* $R_0 > 1$.

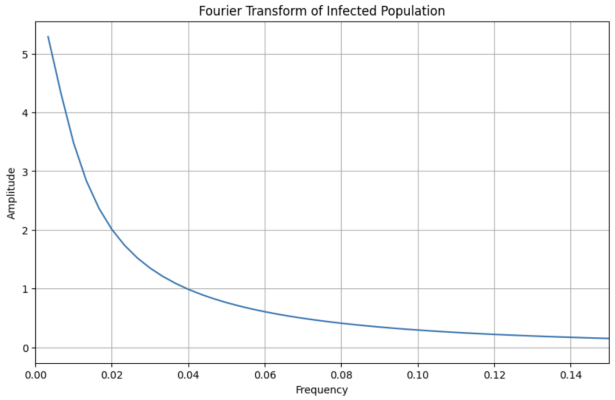

Figure 23 *Fourier Transform SEIR Model - Non-Epidemic scenario with* $R_0 > 1$.

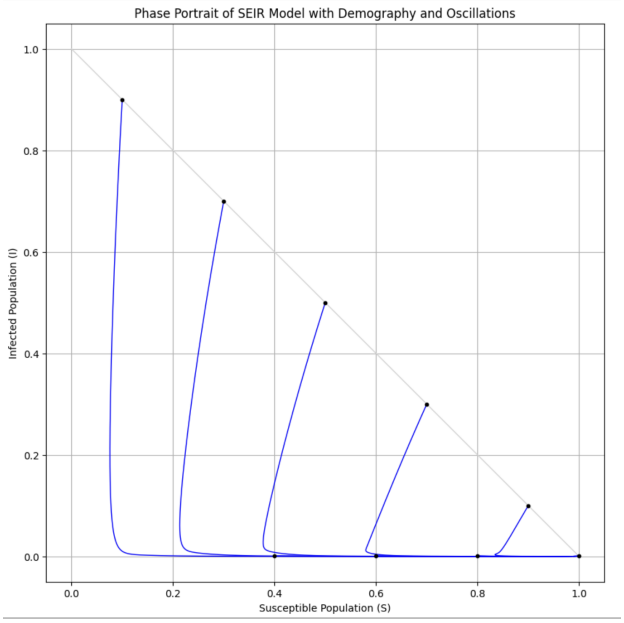

Figure 24 *Phase Portrait SEIR Model - Non-Epidemic scenario with* $R_0 < 1$.

The phase portrait for the non-epidemic scenario, shown in *Figure 23*, presents a similar trajectory to that seen in *Figure 12*, where the disease fails to spread, and eventually, the entire population returns to the susceptible state due to natural causes. Over time, both the infected (I) and recovered (R) populations diminish, leaving the population predominantly in the susceptible (S) category. This phase portrait also reveals fixed points, representing equilibrium states where the populations stabilize. The fixed point at $S = 1$ and $I = 0$ indicates a disease-free equilibrium, where the infection has fully disappeared from the population. Other trajectories tend to converge towards these fixed points, showing how the infection gradually declines and disappears from the population. This pattern is characteristic of models lacking oscillations, reaffirming that the infection will eventually die out under such conditions [11].

4.3 Seasonality

Incorporating seasonality into the SEIR Model allows us to examine the impact of seasonality on the transmission dynamics of the disease [1]. Seasonal changes often influence contact rate and susceptibility to diseases, subsequently having an effect on the disease spread. The modification of the SEIR Model to include seasonality introduces a time-dependent transmission rate (sinusoid) [1], $\beta(t)$, which varies according to the following equation:

$$\beta(t) = \beta_0 \left(1 + \beta_1 \cos\left(\frac{2\pi t}{365}\right)\right)$$

where:

- β_0 represents the average transmission rate over the year,
- β_1 quantifies the amplitude of seasonal variation in the transmission rate, and
- t denotes the time in days, with a period of 365 days assumed for the annual cycle.

This time-dependent transmission rate is incorporated into the SEIR Model equations as follows:

$$\frac{dS}{dt} = \mu(1-S) - \beta(t)SI \tag{1}$$
$$\frac{dE}{dt} = \beta(t)SI - (\sigma+\mu)E \tag{2}$$
$$\frac{dI}{dt} = \sigma E - (\gamma+\mu)I \tag{3}$$
$$\frac{dR}{dt} = \gamma I - \mu R \tag{4}$$

These modified equations account for the effect of seasonality by varying the contact rate between susceptible and infected individuals over time. Such modifications are necessary for the modeling of diseases with clear seasonal patterns.

Figure 25 showcases the dynamics when seasonality

is added to the SEIR Model [17]. In this model, the transmission rate β(t) oscillates annually, leading to corresponding fluctuations in the proportions of susceptible, exposed, infected, and recovered individuals over time. The seasonal peak in the transmission rate, typically coinciding with colder months [10], results in clear waves of infection, which are evident from the noteworthy increases in the infected population. These peaks are followed by significant declines as the transmission rate decreases, allowing the recovery and susceptible rates to catch up.

Figure 25 *Phase Portrait SEIR Model - Non-Epidemic scenario with 1.*

Each wave is characterized by a rapid growth in the Exposed and Infected classes, quickly followed by recovery, due to the natural progression of the disease and demography. This model shows the cyclical nature of diseases known for seasonality, showing that the timing and amplitude of disease outbreaks can often be affected by changes in seasons (and our behavior during those seasons) [2].

5 Conclusion

This paper explored the foundational SIR Model and some variations on the SIR Model to assess how modifications to the Naive SIR framework can improve the understanding (and therefore the management) of infectious disease outbreaks. Through an exploration of the Naive SIR, Generalized SIR, and SEIR Models, we have highlighted the adaptability of mathematical models to accommodate real-world complexities such as vaccination strategies, demographic dynamics, and seasonal influences. The results from each chapter offer an analysis that addresses the research question and its sub-questions.

The Naive SIR model, as discussed in *Chapter 2*, provides a simple framework for understanding the dynamics of infectious disease outbreaks. This model simulates the rapid spread of infections when $R_0 > 1$ and shows the decline of disease when transmission is controlled or natural immunity is established. Answering our first research question:

(1) *How does the Naive SIR model describe the dynamics of an infectious disease, and what are the implications of various vaccination strategies on the model's predictions for epidemic control?*

While the model is useful in understanding the basic disease progression, it falls short of capturing more nuanced aspects of disease spread, such as natural births, deaths, seasonality, and more. *Chapter 2* demonstrated that vaccination strategies, including ring vaccination and contact network strategies, could significantly alter the course of an epidemic, reducing both the peak infection rate and the overall duration of outbreaks. The Naive SIR Model offers a real solid foundation for understanding disease dynamics but would often require further adaptation for practical applications.

In *Chapter 3*, the Generalized SIR model introduced demographic factors such as birth and death rates, along with infection-induced mortality. This extension was essential for understanding how population turnover and disease-induced deaths affect the persistence and oscillations of disease in a population. Answering our second research question:

(2) *How does incorporating demographic factors and infection-induced mortality alter the predictions of the Generalized SIR model?*

This chapter revealed that incorporating demographic stability, especially with constant birth and death rates, can lead to an endemic equilibrium where the disease remains present but does not explode suddenly. The model also demonstrated that infection-induced mortality significantly alters the epidemics life, particularly by shortening the duration of outbreaks when

mortality rates are high. These insights directly answer the second sub-question, confirming that the Generalized SIR model offers a more realistic prediction of disease persistence.

Finally, *Chapter 4* introduced the SEIR model, which added an 'Exposed' class to represent individuals who are infected but not yet infectious. This addition allowed for the modeling of diseases with incubation periods and provided a more refined prediction of infection waves over time. The SEIR model further extended the analysis by incorporating seasonal effects, showing that seasonal variations in transmission rates can lead to periodic outbreaks even in otherwise stable populations. These oscillations, caused by fluctuations in the transmission rate due to environmental or behavioral factors, reflect the cyclical nature of diseases such as influenza. The results of this chapter directly answer the third sub-question:

(3) *What are the dynamics and predictive capabilities of the SEIR Model on infection rates, and what does the addition of seasonal effects change?*

Chapter 4 illustrated that both the Exposed class and seasonal forcing significantly alter the predictive capabilities of the SEIR model, making it a useful Model for modeling diseases with incubation periods and seasonal patterns.

In conclusion, this paper set out to answer our main research question:

How can modifications to the Naive SIR model improve the understanding and management of infectious disease outbreaks?

This paper has demonstrated that modifications to the Naive SIR model (whether by adding vaccination strategies, demographic factors, or seasonal effects) significantly improve our understanding and management of infectious diseases. The enhanced models, such as the Generalized SIR and SEIR frameworks, offer more accurate predictions of disease dynamics, the potential for outbreaks, and the timing of infection waves, particularly in complex epidemiological scenarios. As such, these more-nuanced models can provide useful tools for researchers, allowing for the research of more effective strategies in disease prevention and long-term management.

6 Discussion

While this study demonstrates the theoretical power of the SIR Model, it is important to reflect on the limitations of this model and how these might affect the applicability of the results in real-world settings.

(1) One of the primary limitations of this study is the assumption of homogeneity within the population. All models in this paper assume that individuals mix uniformly, which is rarely the case in real populations where contact patterns are heterogeneous [16]. Therefore, the simplifications used in this study may lead to an over- or under-estimation of the disease's spread in more complex real-world settings.

(2) Another limitation is the lack of stochastic elements in the models. Infectious diseases are inherently stochastic processes where random events can greatly influence the outbreak's progression [4]. By using deterministic models, we lose the ability to simulate the variability that may occur in small populations or early-stage outbreaks. Stochastic models or agent-based simulations could provide a more robust framework to capture these random fluctuations.

(3) In terms of the mathematical framework itself, while modifications such as demographic factors and seasonality were introduced, more advanced features like spatial dynamics and behavioral responses to disease were not incorporated. The extensions we picked now were meant as a good base, but the amount of extensions is seemingly limitless, and new variations on the SIR Model are always actively under development [10]. Other extensions could also offer valuable insights into the spread of diseases and the effectiveness of interventions in real-world scenarios. Future work could explore how adding (e.g.) spatial models, individual movement, and real-time policy interventions impact the course of an epidemic.

In conclusion, while this study demonstrates the adaptability and applicability of the

(Naive/Generalized/Extended) SIR Model in understanding disease dynamics, there remain opportunities for improvement. Future research could focus on addressing these limitations by incorporating heterogeneity, stochastic elements, and more modified factors, ensuring that the models better align with real-world complexities.

References

[1] Z. Bai, Y. Zhou, and T. Zhang. "Existence of multiple periodic solutions for an SIR model with seasonality". In: *Nonlinear Analysis: Theory, Methods & Applications* 74 (18 2011), pp. 7241–7252.

[2] M.H.A. Biswas and L.T. Paiva. "A SEIR model for control of infectious diseases with constraints". In: *Biosciences and Engineering* (2014). URL: https://aimsciences.org.

[3] M. Cerna and A. F. Harvey. "The fundamentals of FFT-based signal analysis and measurement". In: *Citeseer* (2000). URL: https://citeseer.ist.psu.edu.

[4] RAND Corporation. "Targeting High-Contact Individuals in Epidemic Control". In: *RAND Journal of Health* 22 (2020), pp. 110–122. URL: https://www.rand.org/pubs/research_reports/RRxxxx.html.

[5] Frank Fenner. "Smallpox and Its Eradication". In: *World Health Organization* 6 (1988), pp. 125–134.

[6] W. Hamer. "The Dynamics of Epidemic Sprawl". In: *Epidemiological Review* 4 (1897), pp. 45–53.

[7] Herbert W. Hethcote. "The Mathematics of Infectious Diseases". In: *SIAM Review* 42.4 (2000), pp. 599–653.

[8] Özlem İlhan and Gönül Şahin. "A numerical approach for an epidemic SIR model via Morgan-Voyce series". In: *International Journal of Mathematics and Computer* (2024). URL: https://sciendo.com.

[9] Matt J. Keeling and Pejman Rohani. "Chapter 1". In: *Modelling Infectious Diseases in Humans and Animals*. Princeton, NJ: Princeton University Press, 2008. Chap. 1.

[10] Matt J. Keeling and Pejman Rohani. "Chapter 2". In: *Modelling Infectious Diseases in Humans and Animals*. Princeton, NJ: Princeton University Press, 2008. Chap. 2.

[11] Matt J. Keeling and Pejman Rohani. "Chapter 5". In: *Modelling Infectious Diseases in Humans and Animals*. Princeton, NJ: Princeton University Press, 2008. Chap. 5.

[12] A. Perisic and C.T. Bauch. "Social contact networks and disease eradicability under voluntary vaccination". In: *PLoS Computational Biology* (2009). URL: https://journals.plos.org.

[13] E. Ransom. "Historical Epidemiology". In: *Journal of Historical Medicine* 5 (1880), pp. 123–130.

[14] Marcel Salathé and James H. Jones. "Dynamics and control of diseases in networks with community structure". In: *PLoS Computational Biology* 6 (2010), e1000736.

[15] P. Singh and A. Gupta. "Generalized SIR (GSIR) epidemic model: An improved framework for the predictive monitoring of COVID-19 pandemic". In: *ISA Transactions* (2022). URL: https://www.elsevier.com/.

[16] WHO Ebola Response Team. "Ring vaccination with rVSV-ZEBOV under expanded access in response to an Ebola outbreak in Guinea, 2015". In: *The Lancet* 386 (2015), pp. 855–866.

[17] L. Vassallo et al. "Ring vaccination strategy in networks: A mixed percolation approach". In: *Physical Review E* (2020).

[18] H. H. Weiss. "The SIR model and the foundations of public health". In: *Materials Matematics* (2013). URL: https://ddd.uab.cat.

[19] W. Xu, S. Su, and S. Jiang. "Ring vaccination of COVID-19 vaccines in medium-and high-risk areas of countries with low incidence of SARS-CoV-2 infection". In: *Clinical and Translational Medicine* (2021). URL: https://ncbi.nlm.nih.gov.